trans-β-Nitrostyrene Derivatives as Slow-Binding Inhibitors of Protein Tyrosine Phosphatases†

Junguk Park and Dehua Pei*

Department of Chemistry and Ohio State Biochemistry Program, The Ohio State University, 100 West 18th Avenue, Columbus, Ohio 43210

Received June 30, 2004; Revised Manuscript Received August 24, 2004

ABSTRACT: Protein tyrosine phosphatases (PTPs) catalyze the hydrolysis of phosphotyrosyl (pY) proteins to produce tyrosyl proteins and inorganic phosphate. Specific PTPs inhibitors provide useful tools for studying PTP function in signal transduction processes and potential treatment for human diseases such as diabetes, inflammation, and cancer. In this work, *trans*-β-nitrostyrene (TBNS) and its derivatives are found to be slow-binding inhibitors against protein tyrosine phosphatases PTP1B, SHP-1, and Yop with moderate potencies ($K_I^* = 1-10\ \mu M$). Competition experiments with a substrate (*p*NPP) and iodoacetate indicate that TBNS is active site-directed. The mechanism of inhibition was investigated by UV−vis absorption spectroscopy, $^1H-^{13}C$ heteronuclear single-quantum correlation NMR spectroscopy, and site-directed mutagenesis. These studies suggested a mechanism in which TBNS acts a pY mimetic and binds to the PTP active site to form an initial noncovalent E·I complex, followed by nucleophilic attack on the TBNS nitro group by Cys-215 of PTP1B to form a reversible, covalent adduct as the tighter E·I* complex. TBNS derivatives represent a new class of neutral pY mimetic inhibitors of PTPs.

Reversible phosphorylation of proteins on tyrosine residues is one of the key events in cellular signal transduction. The levels of tyrosyl phosphorylation inside a cell are tightly regulated by the opposing actions of two families of enzymes, protein tyrosine kinases (PTKs) and protein tyrosine phosphatases (PTPs).[1] PTPs belong to an extended family of enzymes, and >100 distinct PTPs have already been discovered in the human genome (*1*). However, the study of the physiological functions of these PTPs has lagged behind, due to a lack of effective tools for tackling these problems. Specific, cell membrane-permeable PTP inhibitors would likely provide such tools for studying the function of these enzymes. In addition, a variety of studies have implicated several PTPs as proper targets for the treatment of human diseases and conditions (e.g., PTP1B as a target for treating type 2 diabetes) (*2*−*4*). Thus, PTP inhibitors could also provide potential therapeutic agents.

A large number of PTP inhibitors have been reported in recent years, as a result of intense efforts from both academic and industrial laboratories (see ref *5* for a recent review). Since the substrate of a PTP is a phosphotyrosyl (pY) peptide/protein, a rationally designed PTP inhibitor generally contains two components, a metabolically stable mimetic of pY that interacts with the highly conserved PTP active site and an isostere of the peptide that interacts with the less conserved surfaces near the active site. Most of the reported pY mimetics are negatively charged species, such as phosphonates, malonates, sulfonates, oxalates, and carboxylates (*5*). These negatively charged pY mimetics generally have poor membrane permeability and therefore require prodrug strategies for improving their cellular uptake. In recent years, we have focused our efforts on the development of neutral pY mimetics as PTP inhibitors. We have previously demonstrated that α-haloacetophenone derivatives and peptidyl aldehydes act as covalent PTP inhibitors by reacting with conserved active site residues, the catalytic cysteine (Cys-215 in PTP1B) and arginine (Arg-225 in PTP1B), respectively (*6*−*9*). Here, we report that *trans*-β-nitrostyrene (TBNS) derivatives (Figure 1, compounds **1**−**7** and **9**) act as slow-binding, reversible inhibitors of PTPs. Mechanistic studies suggest that TBNS directly interacts with the active site cysteine residue to form a covalent enzyme−TBNS adduct.

MATERIALS AND METHODS

General. All chemicals used for peptide synthesis were from Advanced ChemTech (Louisville, KY). 1-Phenyl-2-nitroethane was purchased from APIN Chemical, whereas all nitrostyrene derivatives and other chemicals were obtained from Sigma-Aldrich. *Yersinia* PTP Yop and alkaline phosphatase were purchased from New England Biolabs (Beverly, MA). Protein concentrations were determined with a Bradford assay using bovine serum albumin as the standard.

Site-Directed Mutagenesis. Plasmid pET-22(b)-PTP1B was generated by inserting a PCR fragment that encodes amino acids 1−321 of PTP1B into the *Nde*I and *Xho*I site of vector pET-22b (Novagen, Madison, WI). Site-directed mutagenesis

† This work was supported by a grant from the National Institutes of Health (GM62820).

* To whom correspondence should be addressed: Department of Chemistry, The Ohio State University, 100 West 18th Ave., Columbus, OH 43210. Telephone: (614) 688-4068. Fax: (614) 292-1532. E-mail: pei.3@osu.edu.

[1] Abbreviations: ESI-MS, electrospray ionization mass spectrometry; IDA, iodoacetic acid; TBNS, *trans*-β-nitrostyrene; PTP, protein tyrosine phosphatase; *p*NPP, *p*-nitrophenyl phosphate; pY, phosphotyrosine; HSQC, heteronuclear single-quantum correlation.

10.1021/bi0486233 CCC: $27.50
Published on Web 11/04/2004

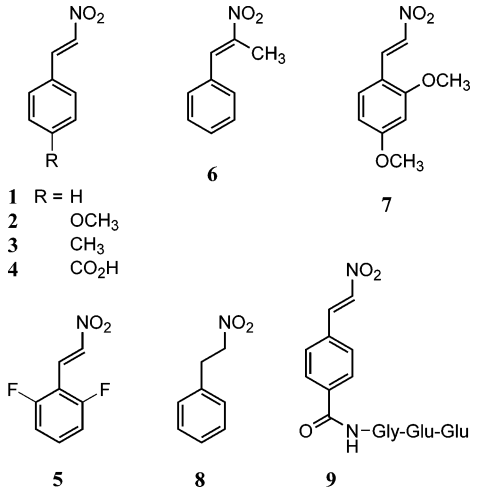

FIGURE 1: Structures of PTP inhibitors.

was carried out with this plasmid DNA as a template using the QuickChange mutagenesis kit (Stratagene, La Jolla, CA). The DNA primers (purchased from Integrated DNA Technologies, Inc.) were as follows: D181A, 5′-TATACCACATGGCCGGCCTTTGGAGT-3′; C215A, 5′-GTTGTGGTGCACGCCAGTGCAGGCATC-3′; C215S, 5′-CCCGTTGTGGTGCACAGCAGTGCAGC-3′; C215D, 5′-CGTTGTGGTGCACGACAGTGCAGGCA-3′; and R225A, 5′-GCAGGCATCGGCGCGTCTGGAACCTTC-3′. The identity of all DNA constructs was confirmed by DNA sequencing. Expression in *Escherichia coli* and purification of recombinant PTP1B were performed as previously described (*10*). The expression and purification of recombinant SHP-1 have also previously been described (*11*).

*Synthesis of 4-Carboxy-trans-β-nitrostyrene (**4**)*. 4-Carboxy-TBNS was prepared according to a modified literature method (*12*). Nitromethane (50.8 mg, 0.83 mmol) was added to 4-carboxybenzaldehyde (100 mg, 0.67 mmol) in methanol (5 mL), and the resulting mixture was cooled to 4 °C. KOH (85 mg, 1.5 mmol) was dissolved in 1 mL of methanol, diluted into 5 mL of an ice/water mixture, and slowly added to the mixture described above through a syringe. After addition of the KOH solution, the reaction mixture was stirred for 15 min at 4 °C. The reaction mixture was diluted into 10 mL of an ice/water mixture, and 100 mL of 5 M HCl was slowly added to the reaction mixture. The pale yellow precipitate that formed was collected by filtration and recrystallized from methanol (yield, 21 mg, 16%): ^{1}H NMR (250 MHz, DMSO-d_6) δ 7.81−7.89 (m, 4H, Ar), 8.04 (d, 1H, ArCH═C*H*NO$_2$, J = 13.7 Hz), 8.16 (d, 1H, ArC*H*═CHNO$_2$, J = 13.7 Hz), 13.18 (s, 1H, ArCO$_2$*H*); HREI-MS calcd for $C_9H_7NO_4$ 193.0370, found 193.0328; λ_{max} = 317 nm; $\epsilon = 1.8 \times 10^4$ M^{-1} cm^{-1}.

*Synthesis of 2,6-Difluoro-trans-β-nitrostyrene (**5**)*. Nitromethane (61.04 mg, 0.88 mmol) was added to 2,6-difluorobenzaldehyde (100 mg, 0.70 mmol) in methanol (5 mL), and the resulting mixture was cooled to 4 °C. KOH (49.4 mg, 0.88 mmol) was dissolved in 1 mL of methanol, diluted into 5 mL of ice-cold water, and slowly added to the mixture described above through a syringe. The reaction mixture was stirred for 20 min at 4 °C. The reaction mixture was diluted into 10 mL of ice-cold water, and 100 mL of 5 M HCl was slowly added to the reaction mixture. The pale yellow precipitate that formed was collected by filtration and recrystallized from methanol (yield, 35 mg, 27%): ^{1}H NMR (250 MHz, DMSO-d_6) δ 7.61−7.73 (m, 1H, Ar), 7.31 (t, 2H, Ar, J = 8.8 Hz), 7.91 (d, 1H, ArCH═C*H*NO$_2$, J = 14.0 Hz), 7.99 (d, 1H, ArC*H*═CHNO$_2$, J = 14.0 Hz); HRESI-MS calcd for $C_9H_6NO_2F_2$ 185.0283, found 185.0281.

*Synthesis of N-{p-[(2-Nitroethenyl)benzoyl]}-L-Gly-L-Glu-L-Glu-NH$_2$ (TBNS-GEE) (**9**)*. Tripeptide Gly-Glu-Glu-NH$_2$ was synthesized on Rink resin by using standard Fmoc chemistry. Next, 4-carboxy-TBNS (**4**) was coupled to the resin-bound tripeptide by using *O*-benzotriazole-*N*,*N*,*N*′,*N*′-tetramethyluronium hexafluorophosphate (HBTU) and *N*-hydroxybenzotriazole monohydrate (HOBt) as coupling agents. The product (TBNS−GEE) was deprotected and released from the solid support by treatment with 99% trifluoroacetic acid (TFA). Excess TFA was removed under a gentle flow of nitrogen, and the residue was triturated with diethyl ether (5 × 3 mL). HPLC analysis of the crude product showed a purity of >90%: HRESI-MS calcd for $C_{21}H_{25}N_5O_{10}$-Na$^+$ ([M + Na]$^+$) 530.1493, found 530.1474.

*Synthesis of trans-[α-^{13}C]-β-Nitrostyrene (**10**)*. This compound was prepared from [*carbonyl*-^{13}C]benzaldehyde by the same procedure that was described for **5**: ^{1}H NMR (250 MHz, $CDCl_3$) δ 8.01 (dd, 1H, ArC*H*═CHNO$_2$, $^3J_{H-H}$ = 13.7 Hz, $^2J_{C-H}$ = 158 Hz), 7.62−7.42 (m, 6H); HRESI-MS calcd for $C_7{}^{13}CH_7NO_2Na^+$ ([M + Na]$^+$) 173.0403, found 173.0405.

PTP Assay. All assay reaction mixtures (1 mL) contained 50 mM HEPES (pH 7.4), 50 mM NaCl, 1 mM EDTA, 2% DMSO, varying concentrations of the PTP inhibitors, and 0.05−0.1 μM PTP. The mixture was incubated for 2 h at room temperature, and the enzymatic reaction was then initiated by the addition of 10 μL of 100 mM *p*NPP and monitored continuously at 405 nm on a λ20 UV−vis spectrophotometer. The IC_{50} values were determined by plotting the remaining activity as a function of inhibitor concentration, and the K_I* values were obtained by fitting the data to the Michaelis−Menten equation. To obtain the K_I value, the reaction was initiated by addition of enzyme (0.05 μM) as the last component to the reaction mixture described above, which also contained 1.0 mM *p*NPP. The reaction was monitored continuously on the UV−vis spectrophotometer. The initial reaction rates were calculated from the early regions of the reaction progress curves (<30 s) and fitted to the Michaelis−Menten equation to give the K_I value. To determine the rate constant k_6, the enzyme (0.1 μM) was incubated with 0−400 μM inhibitor in 100 μL of the reaction buffer described above for 2 h at room temperature. After that, an aliquot of the mixture (25 μL) was withdrawn and rapidly diluted into 975 μL of the same buffer containing 1.0 mM *p*NPP (without the inhibitor). Reactivation of PTP activity was monitored at 405 nm, and the progress curves were fit to the equation $Abs_{405} = v_s[t - (1 - e^{-k_6 t})/k_6]$, where v_s is the final steady-state velocity (*13*). The rate constant k_5 was calculated using the equation $K_I^* = K_I k_6/(k_5 + k_6)$.

Substrate Protection. PTP1B (0.05 μM) was added to the above assay buffer containing a fixed concentration of TBNS (20 μM) and varying concentrations of *p*NPP (0.5−20 mM). The reactions were continuously monitored at 405 nm, and the pseudo-first-order inactivation rate constants (k_{obs}) were obtained by fitting the individual reaction progress curves to the equation $[P] = v_s t + [(v_i - v_s)/k_{obs}](1 - e^{-k_{obs} t})$ (*13*). The obtained k_{obs} values were then plotted against *p*NPP

concentration according to the equation $k_{obs} = k_{max}/(1 + [p\text{NPP}]/K_M)$.

Competition between TBNS and Iodoacetic Acid. PTP1B (5.5 μM) was incubated for 1 h in the assay buffer described above with or without 100 μM TBNS (no *p*NPP). Next, iodoacetic acid (final concentration of 2 mM) was added to the reaction mixture, and the mixture was incubated for an additional 20 min. An aliquot (10 μL) of the reaction mixture was withdrawn and diluted in 990 μL of the assay buffer containing 10 mM *p*NPP and 1 mM β-mercaptoethanol. The reaction was continuously monitored at 405 nm for ~15 min.

NMR Spectroscopy of [α-^{13}C]TBNS and the [α-^{13}C]-TBNS−PTP1B Complex. All NMR experiments were performed on a Bruker DMX-600 NMR spectrometer equipped with a triple-resonance and three-axis gradient probe at 300 K. The two-dimensional (2D) ^{1}H−^{13}C heteronuclear single-quantum coherence (HSQC) spectra were acquired over a period of 2.5 h using a standard Bruker pulse sequence with sensitivity improvement (*14*, *15*). All samples were dissolved in a buffer containing 10 mM HEPES (pH 7.2), 150 mM NaCl, and 1 mM EDTA (10:1 H_2O/D_2O) and preincubated for 1 h at room temperature prior to NMR analysis. The spectral widths were 7184 Hz in the ^{1}H dimension and 21 129 Hz in the ^{13}C dimension, with carrier frequencies at 4.7 and 150 ppm.

RESULTS

Inhibition of PTPs by TBNS and Its Derivatives. A previous study showed that *trans*-cinnamic acid acts as a pY mimetic and, when attached to a Gly-Glu-Glu tripeptide, resulted in potent inhibition versus PTP1B (*16*). More recently, we showed that cinnamaldehyde also acts as a neutral pY mimetic, inhibiting PTPs (*8*), dual-specificity phosphatases (*9*), and Src homology 2 (SH2) domains (*17*). We realized that TBNS (Figure 1, compound **1**) is structurally similar to *trans*-cinnamic acid and cinnamaldehyde and may act as an inhibitor of PTPs. Since the nitro group is electronically neutral, TBNS should have the additional advantage of better membrane permeability over the negatively charged *trans*-cinnamic acid. We thus tested TBNS against protein tyrosine phosphatases PTP1B, SHP-1, and *Yersinia* Yop for potential inhibition. Alkaline phosphatase was also tested as a control. Since TBNS reacts readily with free thiols such as β-mercaptoethanol (*18*), we first tested TBNS against PTPs in the absence of any added free thiols. TBNS resulted in potent inhibition of PTP1B, with an IC_{50} of 2.5 μM (Table 1), which is 10-fold more potent than the negatively charged *trans*-cinnamic acid ($IC_{50} \cong 20$ μM, data not shown). It also inhibited Yop with similar potency ($IC_{50} = 5$ μM) but not alkaline phosphatase. To determine whether the observed inhibition is general for other TBNS derivatives, we tested several commercially available as well as synthetic TBNS derivatives (Figure 1, compounds **2**−**7**), which are modified with either electron-donating (**2**, **3**, and **7**) or electron-withdrawing groups (**4** and **5**) on the phenyl ring. All of the TBNS derivatives inhibited PTP1B, with potencies comparable to that of parent compound **1** (Table 1). In an attempt to improve the inhibitor potency, the Gly-Glu-Glu tripeptide was attached to the para position of TBNS to give the TBNS−GEE species (compound **9**). TBNS−GEE has slightly improved potency ($IC_{50} = 1.4$ μM against PTP1B).

Table 1: Inhibition Constants of TBNS Derivatives against PTP1B and SHP-1(ΔSH2)

	IC_{50} (μM)		
	PTP1B		SHP1(ΔSH2)
inhibitor	no β-mercaptoethanol	with 1 mM β-mercaptoethanol	with 1 mM β-mercaptoethanol
1	2.5 ± 0.3	400 ± 133	423 ± 82
2	4.5 ± 0.5	270 ± 120	375 ± 75
3	3.0 ± 0.5	225 ± 25	~340
4	2.7 ± 0.2	425 ± 75	~450
5	4.8 ± 0.2	~340	ND[b]
6	23 ± 7	515 ± 65	225 ± 75
7	28 ± 8	390 ± 90	~450
8	NA[a]	NA[a]	NA[a]
9	1.4 ± 0.4	275 ± 25	~350

[a] No detectable inhibitory activity. [b] Not determined.

This result suggests that TBNS binds PTPs in a manner different from that of cinnamic acid or cinnamaldehyde. However, it should be possible to convert TBNS into highly potent and selective PTP inhibitors by conjugating it to other peptides, peptidomimetics, or small molecules.

An assay against the catalytic domain of SHP-1, SHP-1(ΔSH2) (*11*), in the absence of free thiol was not possible, because this enzyme was rapidly inactivated under such conditions, presumably due to oxidation of its active site cysteine. We therefore tested the TBNS derivatives against SHP-1(ΔSH2) in the presence of 1 mM β-mercaptoethanol. All of the compounds exhibited inhibition, albeit with much lower potency ($IC_{50} = 200-450$ μM) (Table 1). When PTP1B was tested in the presence of 1 mM free thiol, similar IC_{50} values were obtained. This suggests that the poorer potency observed with SHP-1(ΔSH2) is likely due to thiol inactivation of the TBNS derivatives. To test this notion, we examined the reaction of TBNS with β-mercaptoethanol by monitoring its absorption spectrum on a UV−vis spectrophotometer. In the absence of free thiol, TBNS absorbed strongly at 320 nm and the absorption signal is quite stable (Figure 2A). Upon addition of ~1 equiv of β-mercaptoethanol, the absorption maximum at 320 nm dramatically decreased (Figure 2b). The absorption peak largely disappeared when 2 equiv of thiols was added. However, further addition of excess $HgCl_2$ restored the signal at 320 nm, whereas $HgCl_2$ alone had no effect. These results are consistent with an earlier report that TBNS undergoes reversible conjugate addition with free thiols (Figure 2C), which results in the loss of conjugation between the nitro group and the phenyl ring and therefore the absorption peak at 320 nm (*18*). Moreover, these results suggest that the conjugate addition product does not inhibit PTPs or is a much poorer PTP inhibitor. Indeed, (2-nitroethyl)benzene (Figure 1, compound **8**) showed no significant inhibition of either PTP at 600 μM (Table 1).

Slow-Binding Inhibition of PTPs by TBNS. Compound **1** was selected for further kinetic characterization. It exhibited time-dependent inhibition toward PTP1B (Figure 3A), which could be due to either slow-binding inhibition or time-dependent enzyme inactivation. However, since the observed inhibition is readily reversible (vide infra), it rules out the possibility of irreversible inactivation. Slow-binding inhibition generally results from the formation of an initial enzyme−inhibitor complex, E·I, which can slowly turn into

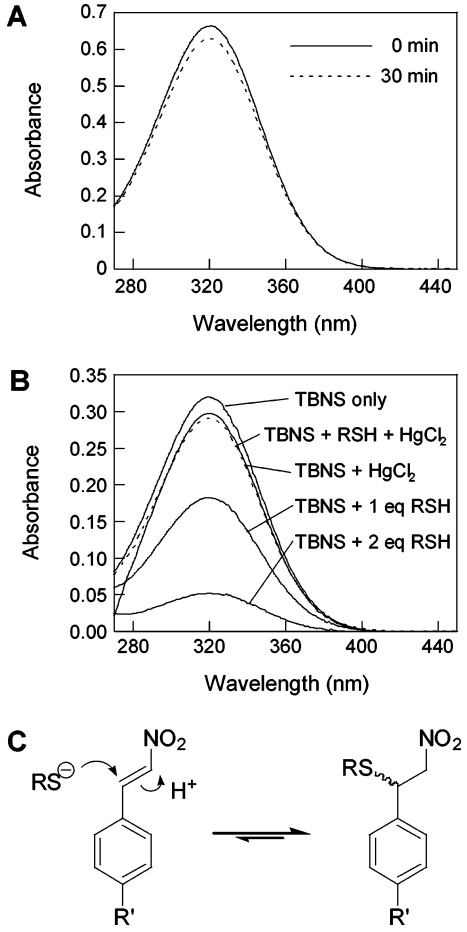

FIGURE 2: Absorption spectra of TBNS in the absence (A) and presence (B) of free thiols. UV−vis absorption of 20 μM of TBNS was monitored in the range of 500−270 nm. All reactions are performed in the assay buffer in the presence of 0, 20, or 40 μM β-mercaptoethanol. An excess of $HgCl_2$ (200 μM) was added to quench β-mercaptoethanol. (C) Reaction of thiols with TBNS.

a tighter enzyme−inhibitor complex, E·I* (*13*). The inhibition kinetics can be described by the equation

$$E + I \overset{K_I}{\rightleftharpoons} E{\cdot}I \underset{k_6}{\overset{k_5}{\rightleftharpoons}} E{\cdot}I^*$$

where K_I is the equilibrium constant for the formation of the initial E·I complex and k_5 and k_6 are the forward and reverse rate constants, respectively, for the conversion of the E·I complex to the tighter E·I* complex. The equilibrium constant K_I* represents the overall potency of the inhibitor, and its relationship with K_I is described by the equation $K_I^* = (K_I k_6)/(k_5 + k_6)$. The K_I and K_I* values of compound **1** against PTP1B were determined to be 150 ± 16 and 1.3 ± 0.2 μM, respectively (see Materials and Methods). To determine whether the inhibition is reversible as well as measuring the k_6 value, PTP1B was preincubated with an excess of TBNS to form the E·I* complex, which was then rapidly diluted into the reaction buffer containing *p*NPP as a substrate. The reaction progress curves as continuously monitored at 405 nm (for the release of *p*-nitrophenolate) showed time-dependent recovery of PTP1B activity (Figure 3b). This result is consistent with the slow-binding mechanism. Curve fitting of the reactivation profiles produced the rate constant k_6 (0.49 min^{-1}). The forward rate constant k_5 was calculated from the K_I, K_I*, and k_6 values (k_5 = 56 min^{-1}). TBNS derivatives **2**−**7** also exhibited slow-binding behavior, although their K_I, K_I*, or k_6 values were not determined.

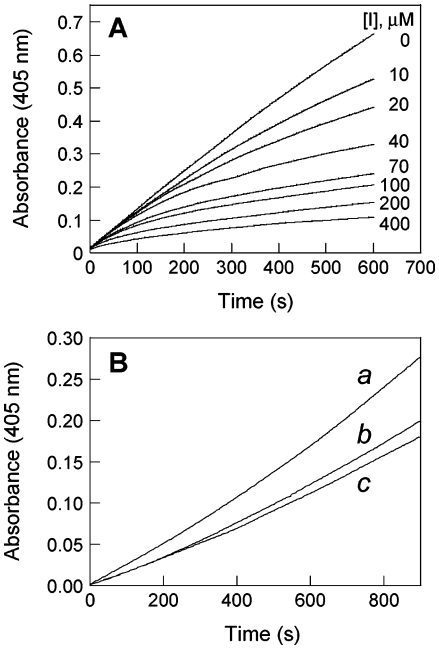

FIGURE 3: Slow-binding inhibition of PTP1B by TBNS. (A) Reaction progress curves (monitored at 405 nm) for the hydrolysis of *p*NPP (1 mM) by PTP1B (0.05 μM) in the presence of indicated concentrations of TBNS (PTP1B was added as the last component). (B) Reaction progress curves for hydrolysis of *p*NPP by reactivated PTP1B. PTP1B (0.1 μM) was preincubated with varying concentrations of TBNS (0−400 μM) for 2 h before being diluted 40-fold into a reaction buffer containing 1.0 mM *p*NPP: (A) 20 μM TBNS, (B) 40 μM TBNS, and (C) 50 μM TBNS.

TBNS Is Active Site-Directed. Two experiments were performed to determine whether TBNS is active site-directed. First, substrate protection was tested by measuring k_{obs}, the pseudo-first-order rate constant for the onset of inhibition, at a fixed inhibitor concentration (20 μM) while varying the *p*NPP concentration (0.5−20 mM). There was clearly an inverse correlation between k_{obs} and *p*NPP concentration (Figure 4A). This result indicates that TBNS and *p*NPP compete for binding to the PTP1B active site. Second, TBNS was tested for its ability to protect PTP1B from covalent modification by iodoacetate (IDA). IDA had previously been shown to selectively alkylate the active site cysteine of PTPs (Cys-215 in PTP1B), causing their irreversible inactivation (*19*, *20*). PTP1B (5.5 μM) was preincubated with TBNS (100 μM) for 1 h prior to the addition of IDA (final concentration of 2 mM). After 20 min, an aliquot of the reaction mixture (10 μL) was diluted 100-fold into an assay buffer containing *p*NPP (1 mM) and β-mercaptoethanol (1 mM) and the reaction progress curve was monitored at 405 nm. Control reactions were carried out with either TBNS or IDA alone. The control reaction with IDA alone produced a linear progress line; its slope indicated a constant remaining PTP activity of 18 μmol mg^{-1} min^{-1} (no PTP reactivation) (Figure 4B). The TBNS only control exhibited slow enzyme reactivation, as observed previously (Figures 3B), and a much higher final PTP activity (93 μmol mg^{-1} min^{-1} at 800 s). The reaction with both TBNS and IDA also exhibited time-dependent reactivation, with a specific PTP activity approaching 75 μmol mg^{-1} min^{-1} at 800 s. The simplest

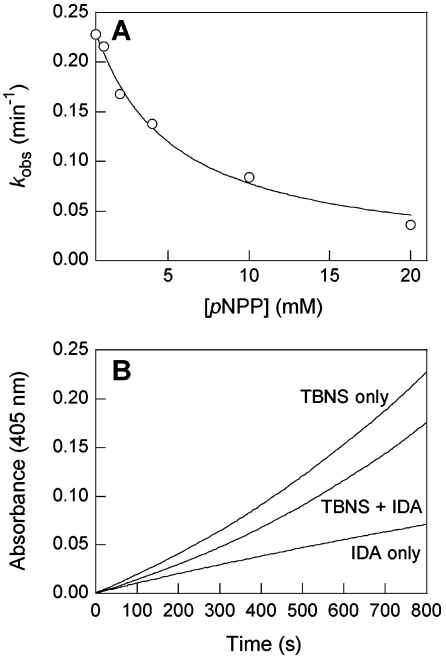

FIGURE 4: Competition for PTP binding between TBNS and *p*NPP or IDA. (A) Effect of substrate concentration on the rate of onset of PTP inhibition by TBNS. The line was fitted to the data according to the equation $k_{obs} = k_{max}/(1 + [pNPP]/K_M)$. (B) Protection of PTP1B from IDA-mediated inactivation by TBNS. PTP1B (5.5 μM) was preincubated with TBNS (100 μM) for 1 h before IDA (final concentration of 2 mM) was added. After 20 min, the remaining PTP activity was assayed with *p*NPP (10 mM) as the substrate.

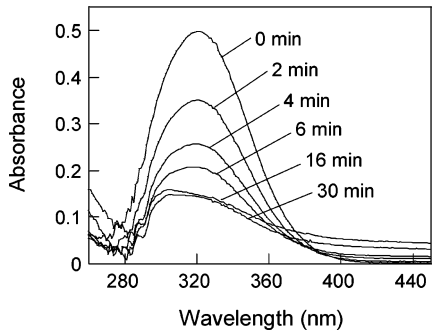

FIGURE 5: Effect of PTP1B on the absorption spectra of TBNS. PTP1B (40 μM) and TBNS (50 μM) were rapidly mixed in a quartz cuvette, and the absorption spectra of the mixture were recorded every 2 min.

explanation for these results is that TBNS bound to the PTP1B active site, preventing its covalent inactivation by IDA. Upon dilution, TBNS dissociated from the PTP active site, restoring the enzymatic activity. Thus, the data given above build a compelling case that TBNS inhibits PTP1B by binding to its active site.

Electronic Absorption Spectroscopy of the E·I Complex*. The mechanism of PTP1B inhibition by TBNS was first examined by UV−vis absorption spectroscopy. PTP1B (39 μM) and TBNS (50 μM) were rapidly mixed in a quartz cuvette, and the absorption spectra were recorded every 2 min. At time 0 (or in the absence of PTP1B), TBNS produced a strong absorption peak at 320 nm (Figure 5). The peak intensity decreased dramatically with time and reached a minimum at 16 min, with a concomitant blue shift of the absorption maximum to ~300 nm. This spectral change occurred on a time scale similar to that of the formation of the E·I* complex, suggesting that formation of the E·I* complex results in the loss of conjugation between the nitro group and the rest of the π system in TBNS. Note that the reaction of TBNS with free thiols also causes the loss of the 320 nm signal (Figure 2). However, the reaction of TBNS with free thiols occurred at a much faster rate and did not result in any blue shift.

^{1}H−^{13}C HSQC NMR Spectroscopy of the E·I Complex*. The nature of the E·I* complex was next examined by ^{1}H−^{13}C HSQC NMR spectroscopy. TBNS containing a specific ^{13}C label at its benzylic position, [α-^{13}C]TBNS (compound **10**), was chemically synthesized. When dissolved in the PTP assay buffer (pH 7.4), [α-^{13}C]TBNS alone exhibited three cross-peaks, which all have the same ^{13}C chemical shift (δ 142.5) but different ^{1}H chemical shift values (δ 8.17, 8.15, and 7.89) (Figure 6A). The doublet at δ 8.17−8.15 represents the cross-peak between the ^{13}C at the α position and the proton directly attached to it; the signal splitting is due to a coupling interaction between the two vinylic protons (J = 13.8 Hz). The cross-peak at δ 7.89/142.5 is caused by long-range coupling between the ^{13}C at position C_α and the vinylic proton at position C_β. These signals were confirmed by 2D heteronuclear shift correlation experiments with ^{13}C directing observation (data not shown). One-dimensional ^{1}H and ^{13}C NMR (carried out in the same buffer), mass spectrometry, and thin-layer chromatography confirmed both the identity and purity of the compound, so the multiple peaks were not caused by the presence of impurities. Upon incubation with a molar excess of PTP1B, all of the free inhibitor signals were lost. Instead, three new, broader cross-peaks were observed in the region of δ 7.6−7.8 (^{1}H)/130−136 (^{13}C) (Figure 6B). As a control, the HSQC spectrum was recorded for the adduct of [α-^{13}C]TBNS and β-mercaptoethanol under the same conditions. Two cross-peaks were observed at δ ~5.2/~46 and δ ~5.1/~46 but not in the region of δ ~7.7/~133, consistent with the conjugate addition of the thiol group to the C_α position and loss of the C═C group (Figure 6C). These results indicate that PTP1B interacts with TBNS in a manner entirely different from that of β-mercaptoethanol. In fact, the chemical shift values of C_α (δ 130−136) suggest that, in the E·I* complex, C_α of TBNS is still in the sp^2 hybridization state and the C═C bond is retained. The presence of three cross-peaks for the E·I* complex was caused by the fact that the recombinant PTP1B was a mixture of multiple isoforms (see the Discussion).

Effect of Active Site Mutations on the E·I Complex*. PTPs share a highly conserved active site, which contains the signature motif, (H/V)C(X)$_5$R(S/T). The cysteine residue (Cys-215 in PTP1B) is the catalytic nucleophile, whereas the arginine (R221 in PTP1B) is critical for substrate binding and transition-state stabilization (*21*, *22*). In addition, a conserved aspartate (Asp-181 in PTP1B) on a mobile loop acts as a general acid or base during catalysis (*23*, *24*). To test the role of these residues in inhibitor binding, we performed the HSQC experiments described above with D181A, R221A, C215S, and C215A mutant forms of PTP1B. D181A and R221A mutants retained the ability to bind to TBNS and produced the same cross-peaks in their HSQC spectra as wild-type (WT) PTP1B (Figure 7A,B). The weaker HSQC signals suggest that TBNS binds less tightly to these mutants (as compared to WT PTP1B). In contrast, the C215A and C215S mutants failed to exhibit any of the three cross-peaks (Figure 7C). Surprisingly, the peaks corresponding to

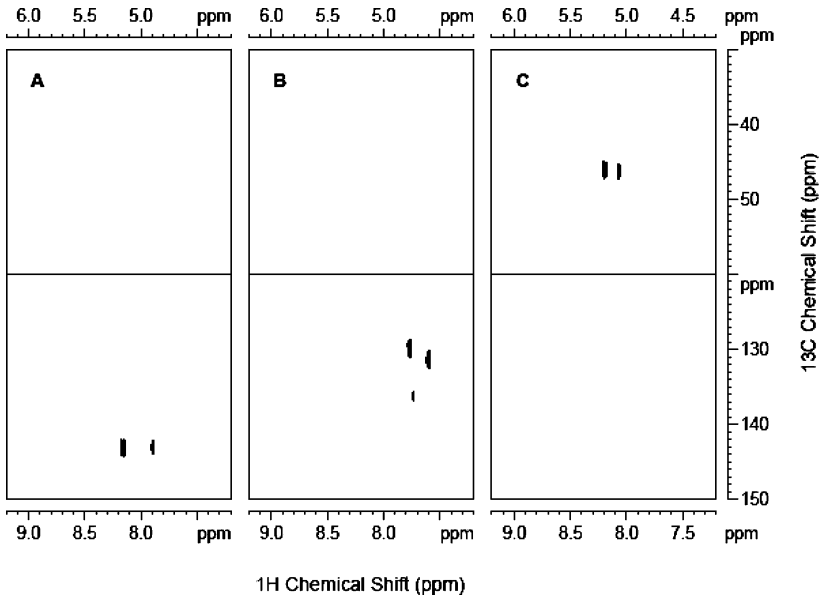

FIGURE 6: HSQC spectra of [α-^{13}C]TBNS (compound **10**) in the absence and presence of PTP1B or free thiol: (A) 600 μM [α-^{13}C]TBNS only, (B) 750 μM [α-^{13}C]TBNS and 1.8 mM PTP1B, and (C) 600 μM [α-^{13}C]TBNS and 2 mM β-mercaptoethanol.

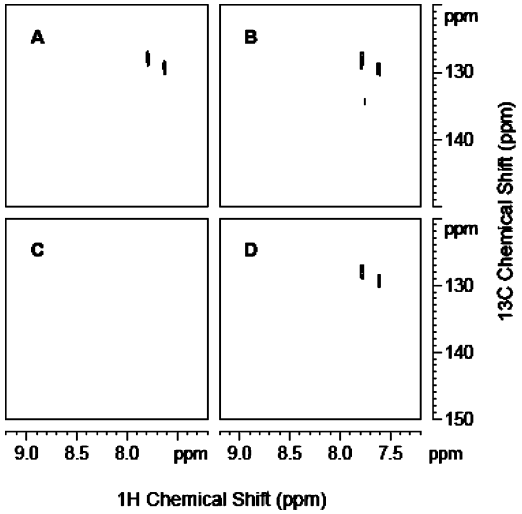

FIGURE 7: HSQC spectra of [α-^{13}C]TBNS (750 μM) in the presence of various PTP1B mutants (each at ~1.5 mM): (A) D181A, (B) R221A, (C) C215S, and (D) C215D.

the free inhibitor were also absent. These results indicate that Cys-215 is critical for TBNS binding; its mutation either abolished inhibitor binding or greatly reduced its binding affinity. The absence of a free inhibitor signal is most likely due to conjugate addition of nucleophilic residues on the PTP1B surface (e.g., cysteines and lysines) to the benzylic position of TBNS. Reaction with multiple residues would scatter the signals to levels beyond detection in the NMR spectra. Electrospray ionization mass spectrometric (ESI-MS) analysis of the mixture of wild-type PTP1B and a molar excess of TBNS showed a major peak at 37 459 (M + 149) and small peaks at 37 605 (M + 298) and 37 756 (M + 447), corresponding to the addition of one, two, and three TBNS molecules, respectively (data not shown). To further evaluate the role of Cys-215, we mutated it into an aspartate. Earlier study has shown that the C215D mutant of PTP1B possesses weak but yet easily detectable catalytic activity toward *p*NPP (*25*). We repeated the HSQC experiment with this mutant and observed two weak peaks at δ ~7.6/~130 and δ ~7.8/~136, the same region where the three cross-peaks were observed for the WT enzyme (Figure 7D). Thus, the C215D mutant also retains the ability to bind TBNS. The same conclusions were also independently reached by ESI-MS analysis of the mutants complexed with TBNS (data not shown).

DISCUSSION

In this work, we have demonstrated that TBNS and its derivatives act as neutral pY mimetics and slow-binding inhibitors of PTPs. In the absence of free thiols or other nucleophilic species that react with the Michael acceptor, these compounds exhibited respectable potency, with IC_{50} values in the low micromolar range. Considering their small sizes, the compounds probably only interact with the PTP active site. Thus, the observed potency is quite remarkable and may be further improved by tethering the pY mimetics to peptides, peptidomimetics, or small molecules that interact favorably with the surfaces near the PTP active site. Since the active site of PTPs is highly conserved and all of the compounds that were tested exhibited essentially equal potencies against PTP1B, SHP-1, and Yop, we expect the TBNS derivatives to be effective against all PTPs. One drawback of the current TBNS derivatives is that they readily react with free thiols (which are present in the cytoplasm of eukaryotic cells) and possibly other nucleophiles, resulting in the dramatic reduction of their PTP inhibitory activity. However, the addition of thiols to TBNS is readily reversible. It may be possible to design TBNS analogues that are less prone to nucleophilic addition by thiols (e.g., by the substitution of powerful electron-donating groups at the para position) and therefore more available for PTP inhibition.

On the basis of experimental data described above, we propose the following mechanism of inhibition by TBNS (Figure 8). TBNS first binds to the active site of PTP and forms a noncovalent complex, E·I. During the conversion of the E·I complex to the tighter E·I* complex, the active site thiolate anion (Cys-215 in PTP1B) reacts with the nitro group of TBNS to form a covalent adduct. Nucleophilic addition of thiols to aliphatic and aromatic nitro compounds

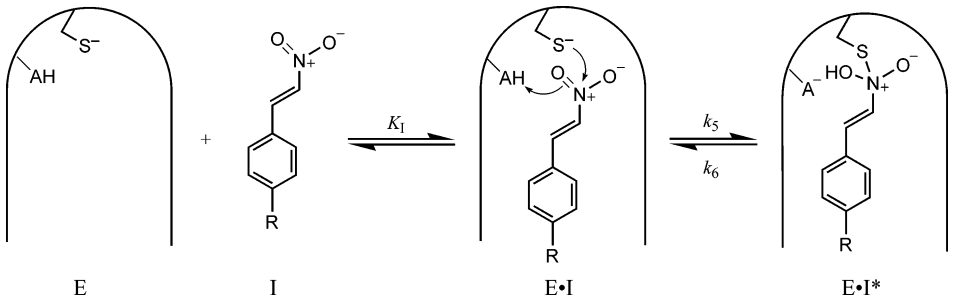

FIGURE 8: Proposed mechanism for the slow-binding inhibition of PTPs by TBNS derivatives.

is well-documented in the literature and is the first step in the Zinin reduction of nitro compounds to their corresponding amines (*26*). This mechanism is consistent with all of the experimental results. First, it provides a sensible explanation for the slow-binding behavior, as the chemical step is reversible and time-dependent. Second, mutation of Cys-215, which is the catalytic nucleophile for the PTP reaction and the proposed nucleophile attacking the nitro group, to either alanine or serine abolished both PTP activity and TBNS binding (Figure 7C). On the other hand, substitution of aspartate for Cys-215 leads to retention of partial catalytic activity (*25*) and the ability to bind TBNS (Figure 7D). This indicates that a powerful nucleophilic side chain at residue 215 is critical for inhibitor binding. In contrast, mutation of two other catalytic residues, Arg-221 and Asp-181, weakened but did not abolish the binding by TBNS (Figure 7A,B). Third, HSQC spectra of the E·I complex revealed cross-peaks at δ ~7.7/132. The ^{13}C chemical shift values indicate that the C_α atom is still in the sp^2 hybridization state in the E·I* complex (the C═C bond is intact). Therefore, unlike its reaction with free thiols, binding of TBNS to the PTP1B active site involves no nucleophilic addition to the C═C bond. The upfield shift of the cross-peaks upon binding to PTP1B may be ascribed to the fact that addition of Cys-215 (or Asp-215) to the nitro group reduces the electron-withdrawing ability of the nitrogen and therefore the inductive effect on C_α and its proton.

Why is the C═C bond in TBNS necessary for inhibition if it is not attacked by an enzyme nucleophile? It is possible that the C═C bond maintains a rigid planar geometry which is critical for binding and/or positioning the nitro group for nucleophilic attack. Presumably, loss of the C═C bond (as in **8**) makes binding and nucleophilic attack entropically unfavorable. In this regard, cinnamic acid inhibits PTP1B with an IC_{50} value of ~20 μM (*16*), whereas 3-phenylpropionic acid is not known to have any inhibitory activity against the enzyme. Likewise, while cinnamaldehyde inhibits PTP1B with an IC_{50} value of 970 μM (*8*), 3-phenylpropanal exhibits no measurable inhibition of any PTP (unpublished results).

The mechanism described above does not explain the presence of three cross-peaks in the HSQC spectra. Since the three cross-peaks of the PTP1B−TBNS complex have different ^{13}C chemical shift values, they cannot be caused by the same signal splitting that was observed for free TBNS. Moreover, in a high-molecular weight complex such as the PTP1B−TBNS adduct, signal splitting is usually not observed due to peak broadening. We noticed that these cross-peaks are remarkably similar to those produced by the E·I* complex formed by PTP1B and peptidyl cinnamaldehyde inhibitors (*8*). In the latter case, the cinnamaldehyde was labeled with ^{13}C at the aldehyde carbonyl and the cinnamaldehyde forms an enamine adduct with active site arginine-221 of PTP1B. It was proposed that the enamine could adopt different diastereomer forms, which gave different HSQC cross-peaks (*8*). However, the E·I* complex formed by PTP1B and TBNS cannot assume these different diastereomeric forms. An alternative explanation is that the recombinant PTP1B protein may be a heterogeneous mixture of multiple species. Two-dimensional SDS−PAGE analysis of freshly prepared PTP1B samples revealed that it contained four different variants, all of which had molecular masses of ~37 kD but different pI values (5.98, 6.09, 6.24, and 6.39) (unpublished results). ESI-MS analysis of the free protein showed four peaks with molecular weights of 37 310, 37 335, 37 354, and 37 435 (unpublished results). Both SDS−PAGE and MS analyses gave a similar estimate for the relative intensities of the four species: 100% for MW = 37 310, 60% for MW = 37 335, 25% for MW = 37 354, and 15% for MW = 37 435. Analysis of multiple PTP1B samples purified at different times reproducibly gave the same pattern. Note that the intensity ratio is similar to that found for the three cross-peaks in the HSQC spectra (Figure 6). The peak at *m*/*z* 37 310 probably represents the unmodified PTP1B (the calculated molecular weight of PTP1B is 37 312), whereas the nature of modification in the other three species is unknown. ESI-MS analysis of the PTP1B−TBNS complexes showed that all four PTP1B variants were capable of binding TBNS.

In conclusion, we have discovered TBNS and its derivatives as a new class of reversible, covalent PTP inhibitors. Its electronically neutral nature may provide good membrane permeability for this class of inhibitors. Further studies for improving their stability against thiols and their potency and selectivity are already underway in this laboratory.

ACKNOWLEDGMENT

We thank Dr. Chunhua Yuan for excellent technical assistance in acquiring the HSQC spectra and Drs. Ming-Tsai, Mark Foster, Charles Cottrell, and Chunhua Yuan for helpful discussions throughout this project.

REFERENCES

1. Alonso, A., Sasin, J., Bottini, N., Friedberg, I., Friedberg, I., Osterman, A., Godzik, A., Hunter, T., Dixon, J., and Mustelin, T. (2004) Protein tyrosine phosphatases in the human genome, *Cell 117*, 699−711.
2. Moller, D. E. (2001) New drug targets for type 2 diabetes and metabolic syndrome, *Nature 414*, 821−827.
3. Ukkola, O., and Santaniemi, M. (2002) Protein tyrosine phosphatase 1B: a new target for the treatment of obesity and associated co-morbidities, *J. Int. Med. 251*, 467−475.

4. Zhang, Z.-Y. (2001) Protein tyrosine phosphatases: prospects for therapeutics, *Curr. Opin. Chem. Biol. 5*, 416−423.
5. Zhang, Z.-Y. (2002) Protein tyrosine phosphatases: structure and function, substrate specificity, and inhibitor development, *Annu. Rev. Pharmacol. Toxicol. 42*, 209−234.
6. Arabaci, G., Guo, X.-C., Beebe, K. D., Coggeshall, K. M., and Pei, D. (1999) α-Haloacetophenone Derivatives as Photoreversible Covalent Inhibitors of Protein Tyrosine Phosphatases, *J. Am. Chem. Soc. 121*, 5085−5086.
7. Arabaci, G., Yi, T., Fu, H., Porter, M. E., Beebe, K. D., and Pei, D. (2002) α-Bromoacetophenone Derivatives as Neutral Protein Tyrosine Phosphatase Inhibitors: Structure−Function Relationship, *Bioorg. Med. Chem. Lett. 12*, 3047−3050.
8. Fu, H., Park, J., and Pei, D. (2002) Peptidyl Aldehydes as Reversible Covalent Inhibitors of Protein Tyrosine Phosphatases, *Biochemistry 41*, 10700−10709.
9. Park, J, Fu, H., and Pei, D. (2004) Peptidyl aldehydes as slow-binding inhibitors of dual-specificity phosphatases, *Bioorg. Med. Chem. Lett. 14*, 685−687.
10. Barford, D., Keller, J. C., Flint, A. J., and Tonks, N. K. (1994) Purification and crystallization of the catalytic domain of human protein tyrosine phosphatase 1B expressed in *Escherichia coli*, *J. Mol. Biol. 239*, 726−730.
11. Pei, D., Neel, B. G., and Walsh, C. T. (1993) Overexpression, Purification, and Characterization of SHPTP1, a Src Homology 2-Containing Protein-Tyrosine-Phosphatase, *Proc. Natl. Acad. Sci. U.S.A. 90*, 1092−1096.
12. Ramfry, F. C. P. (1911) The condensation of aromatic aldehydes with nitromethane, *J. Chem. Soc. 79*, 282−288.
13. Morrison, J. F., and Walsh, C. T. (1988) The behavior and significance of slow-binding enzyme inhibitors, *Adv. Enzymol. 61*, 201−301.
14. Kay, L. E., Keifer, P., and Saarinen, T. (1992) Pure absorption gradient enhanced heteronuclear single quantum correlation spectroscopy with improved sensitivity, *J. Am. Chem. Soc. 114*, 10663−10665.
15. Schleucher, M., Schwendinger, M., Sattler, M., Schmidt, P., Schedletzky, O., Glaser, S. J., Sorensen, O. W., and Griesinger, C. (1994) A general enhancement scheme in heteronuclear multidimensional NMR employing pulsed field gradients, *J. Biomol. NMR 4*, 301−306.
16. Moran, E. J., Sarshr, S., Cargill, J. E., Shahbaz, M. M., Lio, A., Mjalli, A. M. M., and Armstrong, R. W. (1995) Radio frequency tag encoded combinatorial library method for the discovery of tripeptide-substituted cinnamic acid inhibitors of the protein tyrosine phosphatase PTP1B, *J. Am. Chem. Soc. 117*, 10787−10788.
17. Park, J., Fu, H., and Pei, D. (2003) Peptidyl Aldehydes as Reversible Covalent Inhibitors of Src Homology 2 Domains, *Biochemistry 42*, 5159−5167.
18. Bernasconi, C. F., and Schuck, D. F. (1992) Kinetics of reversible thiolate ion addition to substituted β-nitrostyrenes in water. Radicaloid transition state or principle of nonperfect synchronization? *J. Org. Chem. 57*, 2365−2373.
19. Zhang, Z.-Y., and Dixon, J. E. (1993) Active site labeling of the *Yersinia* protein tyrosine phosphatase: The determination of the pK_a of the active site cysteine and the function of the conserved histidine 402, *Biochemistry 32*, 9340−9345.
20. Pot, D. A., and Dixon, J. E. (1992) Active site labeling of a receptor-like protein tyrosine phosphatase, *J. Biol. Chem. 267*, 140−143.
21. Zhang, Z.-Y., and Dixon, J. E. (1994) Protein tyrosine phosphatase: Mechanism of catalysis and substrate specificity, *Adv. Enzymol. 68*, 1−36.
22. Zhang, Z.-Y., Wang, Y., Wu, L., Fauman, E. B., Stuckey, J. A., Schubert, H. L., Saper, M. A., and Dixon, J. E. (1994) The Cys(X)$_5$Arg catalytic motif in phosphoester hydrolysis, *Biochemistry 33*, 15266−15270.
23. Zhang, Z.-Y., Wang, Y., and Dixon, J. E. (1994) Dissecting the catalytic mechanism of protein tyrosine phosphatases, *Proc. Natl. Acad. Sci. U.S.A. 91*, 1624−1627.
24. Flint, A. J., Tiganis, T., Barford, D., and Tonks, N. K. (1997) Development of "substrate-trapping" mutants to identify physiological substrates of protein tyrosine phosphatases, *Proc. Natl. Acad. Sci. U.S.A. 94*, 1680−1685.
25. Romsicki, Y., Scapin, G., Beaulieu-Audy, V., Patel, S., Becker, J. W., Kennedy, R. P., and Asante-Appiah, E. (2003) Functional characterization and crystal structure of the C215D mutant of protein-tyrosine phosphatase-1B, *J. Biol. Chem. 278*, 29009−29015.
26. Porter, H. K. (1973) The Zinin reduction of nitroarenes, *Org. React. 20*, 455−481.

BI0486233